

the wave field in the crystal, and resonant amplification of the oscillations of the intensity of the diffracted and transmitted beams with the fundamental period  $\lambda_s$ .

The author thanks V. I. Nikitenko for a useful discussion of the work.

<sup>1)</sup>At  $|a| > \frac{1}{2} \text{Im}(\Delta K_H)$  the degeneracy of the real parts of the eigenvalues is lifted and the branches do not intersect.

<sup>1</sup>K. Haruta, J. Appl. Phys. **38**, 3312 (1967).

<sup>2</sup>R. D. Mindlin and W. J. Spencer, J. Acoust. Soc. Am. **42**, 1268 (1967).

<sup>3</sup>R. Köhler, W. Möhling, and H. Peibst, Phys. Status Solidi B **61**, 439 (1974).

<sup>4</sup>E. J. Saccocio, M. A. Lopez, and K. J. Lazara, J. Appl. Phys. **38**, 309 (1967).

<sup>5</sup>A. Hauer and S. J. Burns, Appl. Phys. Lett. **27**, 524 (1975).

<sup>6</sup>G. Borrmann, Z. Phys. **42**, 157 (1941).

<sup>7</sup>I. R. Éntin, Pis'ma Zh. Eksp. Teor. Fiz. **26**, 392 (1977) [JETP Lett. **26**, 269 (1977)].

<sup>8</sup>I. R. Éntin, E. V. Suvorov, N. P. Kobelev, and Ya. M. Soifer, Fiz. Tverd. Tela (Leningrad) **20**, 1311 (1978) [Sov. Phys.

Solid State **20**, 754 (1978)].

<sup>9</sup>I. R. Éntin, Fiz. Tverd. Tela (Leningrad) **20**, 2130 (1978) [Sov. Phys. Solid State **20**, 1230 (1978)].

<sup>10</sup>I. R. Entin, Phys. Status Solidi B **90**, 575 (1978).

<sup>11</sup>S. Takagi, J. Phys. Soc. Jpn. **26**, 1239 (1969).

<sup>12</sup>A. M. Afanasev, Yu. Kagan, and F. N. Chukhovskii, Phys. Status Solidi **28**, 287 (1968).

<sup>13</sup>R. Köhler, W. Möhling, and H. Peibst, Phys. Status Solidi B **61**, 173 (1974).

<sup>14</sup>J. C. Slater, Insulators, Semiconductors, and Solids, McGraw, 1967.

<sup>15</sup>B. W. Batterman and H. Cole, Rev. Mod. Phys. **36**, 681 (1964).

<sup>16</sup>I. E. Dzyaloshinskii, Zh. Eksp. Teor. Fiz. **47**, 336 (1964) [Sov. Phys. JETP **20**, 223 (1965)].

<sup>17</sup>P. B. Hirsch *et al.*, Electron Microscopy of Thin Crystals, Plenum, 1965 [Russ. transl., Mir, 1968, pp. 266 and 295].

<sup>18</sup>A. V. Kolpakov and Yu. P. Khapachev, Kristallografiya **18**, 474 (1973) [Sov. Phys. Crystallogr. **18**, 300 (1973)].

<sup>19</sup>S. D. Le Roux, R. Colella, and R. Bray, Phys. Rev. Lett. **35**, 230 (1975).

<sup>20</sup>B. Dietrich, Coll. Abstr. of the Eleventh Intern. Congress of Cryst., S230, Warsaw, Poland, 1978.

Translated by J. G. Adashko

## Finite-dimension ring interferometer in an external magnetic field

G. F. Zharkov and A. D. Zaikin

*P. N. Lebedev Physics Institute, USSR Academy of Sciences*

(Submitted 19 January 1979)

Zh. Eksp. Teor. Fiz. **77**, 223-235 (July 1979)

A theory is developed for a single ring interferometer (SQUID) having a finite contact with  $L$  and placed in an external static magnetic field  $H_e$ . Numerical methods are used to study the nonlinear-equation solutions that yield the distributions of the field in the ring and inside the contact. The obtained solutions are investigated for stability, and the stable and unstable configurations are determined. The free energies of the different states are obtained. The points of equilibrium transition from one state to another are found, as are the boundaries of the hysteresis region. The dependence of the field  $H_i$  inside the ring on the external field  $H_e$  is plotted at different values of the width  $L$  of the contact and of the area  $\sigma$  of the internal opening of the ring. In the limiting case of small widths ( $L < 1$ ), and also in the case of strong fields ( $H_e \gg 1$ ), analytic formulas are obtained. The general expression for the self-induction coefficient of the ring interferometer is found. A comparison is made with the results of other studies of this subject.

PACS numbers: 85.25. + k

### 1. INTRODUCTION

We consider in this paper the problem of penetration of an external static magnetic field into a superconducting ring that is closed by a Josephson junction of finite width  $L$  (see Fig. 1). The external magnetic field  $H_e$  is directed along the  $z$  axis perpendicular to the plane of the figure. It is assumed that the superconductor has an infinite length along the  $z$  axis (cylinder with cuts along  $L$ ). It is obvious that all the quantities in the plane of the barrier depend in this case only on the angle coordinate  $x(0 \leq x \leq L)$ .

The distribution of the field and of the current in a

Josephson barrier of finite width is described by the nonlinear equation<sup>1-3</sup>

$$d^2\varphi/dx^2 = \sin \varphi, \quad (1)$$

where the density of the current through the barrier is  $j(x) = \sin \varphi(x)$  and the magnetic field is  $H(x) = d\varphi/dx$ . (The quantity  $\varphi(x)$  is called the phase difference of the superconductor order parameter.)

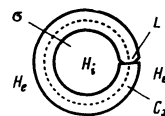


FIG. 1. Schematic view of a ring SQUID in an external field.

The main purpose of the study is to find the field  $H_i$  inside the barrier as a function of the field  $H_e$  on its outer boundary. This problem is timely because systems with ring SQUIDS<sup>1</sup> are widely used for exact measurements of magnetic fields so that an analysis of the operation of such a device is of practical importance. Many papers have been written on this subject, except that the weak link in the superconducting ring is usually assumed to be the point contact (see, e.g., Refs. 1-8), i.e.,  $L \ll 1$ ; we, however, are interested in the case of a barrier of finite width ( $L \geq 1$ ).<sup>2</sup>

To solve our problem it is necessary to formulate the boundary conditions for Eq. (1). One of the conditions is obvious: since the external field is given, we have

$$d\varphi/dx|_{x=L} = H_e. \quad (2)$$

To find the second boundary condition we use the connection between the phase difference  $\varphi(x)$  at some point  $x$  of the barrier and the flux inside the ring (cf. Refs. 1-7):

$$\varphi(x) = \frac{\Phi(x)}{\Phi_0/2\pi}, \quad \Phi(x) = \oint_{C_x} A dl \quad (3)$$

(it is easily seen that the condition (3) takes into account the effect of quantization of the ring). Here  $\Phi_0 = hc/2e = 2 \cdot 10^{-7}$  Oe-cm<sup>2</sup> is the flux quantum,  $\Phi(x)$  is the magnetic field inside the closed contour  $C_x$  passing in the interior of the ring walls and crossing the junction at a certain point  $x$  (see Fig. 1). Recognizing that  $\Phi(0) = H_i \pi r^2$  (we use here dimensional units, with  $r$  the inside radius of the ring), we obtain the sought condition in the form (see also Refs. 9 and 10)

$$\varphi(0) = \sigma \frac{d\varphi}{dx} \Big|_{x=0} = \sigma H_i. \quad (4)$$

Here  $\sigma = \pi r^2 / \lambda_j \Lambda$ ,  $\Lambda = 2\lambda_z + l$  is the effective thickness of the layer in which a magnetic field is present in the junction, and  $H_i$  is the dimensionless field (see footnote 2).

Equation (1) jointly with the boundary conditions (2) and (4) enables us to find the distribution of the field and of the current in the junction, and simultaneously also the value of the field  $H_i$  inside the ring as a function of  $H_e$ ,  $L$ , and  $\sigma$ . To solve our problem we note first that Eq. (1) has a first integral in the form

$$x = \frac{1}{2} \int_{\varphi(0)}^{\varphi(x)} \frac{dy}{\xi R(y)}, \quad R(y) = \left\{ \sin^2 \frac{y}{2} + C \right\}^{1/2} \geq 0, \quad (5)$$

where  $C$  is an arbitrary constant,  $\varphi(0)$  is the value of  $\varphi(x)$  at  $x = 0$ , and  $\xi = \pm 1$  is the sign function. The derivative  $d/dx$  is written in accordance with (5) in the form

$$d\varphi/dx = 2\xi \{ \sin^2(\varphi(x)/2) + C \}^{1/2}. \quad (6)$$

It follows therefore that at  $C > 0$  the derivative  $d\varphi/dx$  [i.e., the field  $H(x)$ ] does not vanish anywhere and the corresponding solution  $\varphi(x)$  varies monotonically with increasing  $x$  (increasing solution at  $\xi = 1$ ).

In the case  $C < 0$  the derivative  $d\varphi/dx$  vanishes at certain points, where it reverses sign (because the solution is continuous). This case corresponds to bounded solutions. For these solutions it is necessary

to take into account in (6) the sign function  $\xi = \pm 1$ , which determines the direction of the field at the given point. The integral (5) enables us to express  $\varphi(x)$  in terms of Jacobi elliptic functions, but we shall find it more convenient to deal directly with the integral representation (5).

## 2. REGIONS OF EXISTENCE AND CLASSIFICATION OF SOLUTIONS

As in a number of preceding papers<sup>11-16</sup> it is convenient to reduce the solution of the boundary-value problem (1) to an investigation of the corresponding Cauchy problem, i.e., to finding the "initial" values  $\varphi(0)$  that determine uniquely, jointly with the initial derivative  $d\varphi/dx|_{x=0} = H_i$ , all the solutions of Eq. (1). Assume that we know the value of the field  $H_i$  which was established inside the ring. The solution  $\varphi(x)$  must in this case satisfy the requirement  $d\varphi/dx|_{x=0} = H_i$ , from which we get, taking (6) into account

$$C = H_i^2/4 - \sin^2(\varphi(0)/2). \quad (7)$$

It is clear therefore that, depending on the ratio of  $H_i$  to  $\varphi(0)$ , the problem can have negative and positive values of  $C$ , i.e., both increasing and bounded solutions.

From condition (2) and the equation  $d\varphi/dx|_{x=L} = H_e$  we obtain with the aid of (6) the relation

$$H_e^2/4 - \sin^2(\varphi(L)/2) = H_i^2/4 - \sin^2(\varphi(0)/2), \quad (8)$$

which serves to determine the values of  $\varphi(L)$ :

$$\begin{aligned} \varphi(L) &= \pm A + 2\pi n, \\ A &= 2 \arcsin \{ (H_e^2 - H_i^2)/4 + \sin^2(\varphi(0)/2) \}^{1/2}. \end{aligned} \quad (9)$$

We chose here for  $A$  the principal value of the arcsine,  $0 \leq A \leq \pi$ , and  $n$  is an arbitrary integer. Substituting the value  $x = L$  in (5) we obtain, taking the foregoing into account, the integral equation

$$L = \frac{1}{2} \int_{\varphi(0)}^{\pm A + 2\pi n} \frac{dy}{\xi R(y)}, \quad (10)$$

which serves to determine the quantities  $\varphi(0)$  as functions of  $L$ ,  $H_e$ ,  $\sigma$ , and the number  $n$ . It must be recognized in (7)-(10) that  $H_i = (0)/\sigma$  in accordance with (4). Knowledge of the quantities  $\varphi|_{x=0} = \varphi(0)$  and  $d\varphi/dx|_{x=0} = H_i$  enables us to determine uniquely the corresponding solution of Eq. (1) and to determine both the magnetic flux that is established in the ring [see (3) and (4)] and the distribution of the field and of the current inside the junction.

Equation (10) was solved numerically with a computer. The results of the investigations are shown in Figs. 2-4, where  $H_i$  is plotted as a function of  $H_e$  for several values of  $L$  and  $\sigma$ . Each point on these curves, given  $H_i$ ,  $L$ , and  $\sigma$  corresponds to fully defined values of  $\varphi(0)$  and  $H_i = \varphi(0)/\sigma$ , i.e., corresponds to a fully defined solution of Eq. (1). To make it easier to follow the qualitative changes of the solution as the representative point moves along the curves of Figs. 2-4, it is convenient to classify the solutions in accord with whether the field inside the ring is larger or smaller than the outside field. Figure 5 shows, in the  $(H_i, H_e)$  plane, the domain of existence of static solutions of Eq. (1), brok-

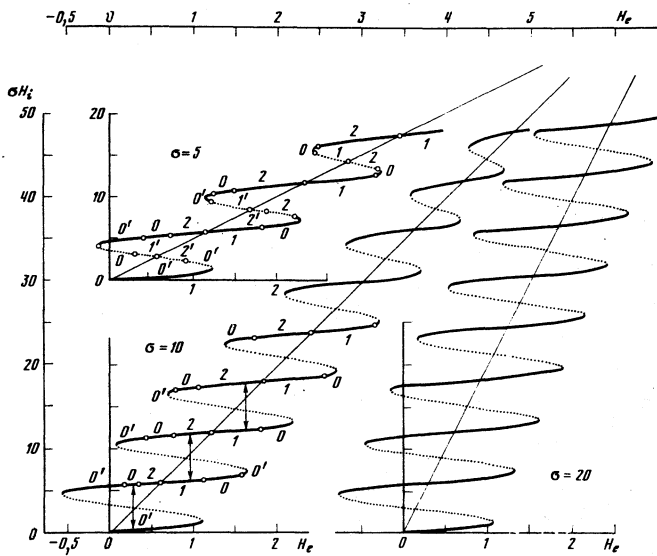


FIG. 2. The flux  $\sigma H_i$  inside the ring vs the external field for a ring SQUID with  $L=1$  and with  $\sigma=5, 10$ , and  $20$ . The thick sections of the curves correspond to stable states, the dotted sections show the unstable states. The numbers on the curves correspond to different field configurations in the junction in accordance with the classification used for the states in Fig. 6.

en up into 12 regions,<sup>3</sup> depending on the relation between  $H_i$  and  $H_e$ . In addition, the boundary  $|H_i| = |H_e| = 2$ , which is a singular line for Eq. (1), is separated and the curves  $H_i = (H_e \pm 4)^{1/2}$ , where  $A = 1$ , are shown. There are no static solutions outside the indicated region.

Equations (9) and (10) contain the integer  $n$  which determines the number of extremal points of the function  $H(x)$  (i.e., the number of vortices inside a junction of width  $L$ ). Figure 6 shows schematically the behavior of  $H(x)$  in regions II–VII (in our problem it suffices to consider the solutions in only these regions). The

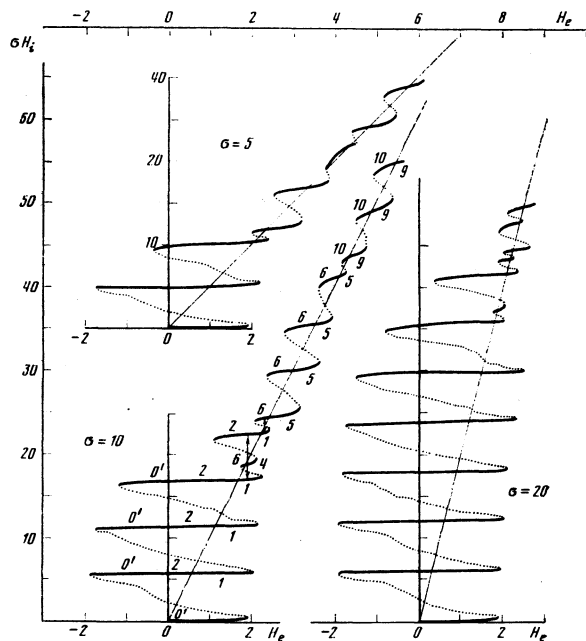


FIG. 3. The same as in Fig. 2, but at  $L=3$ .

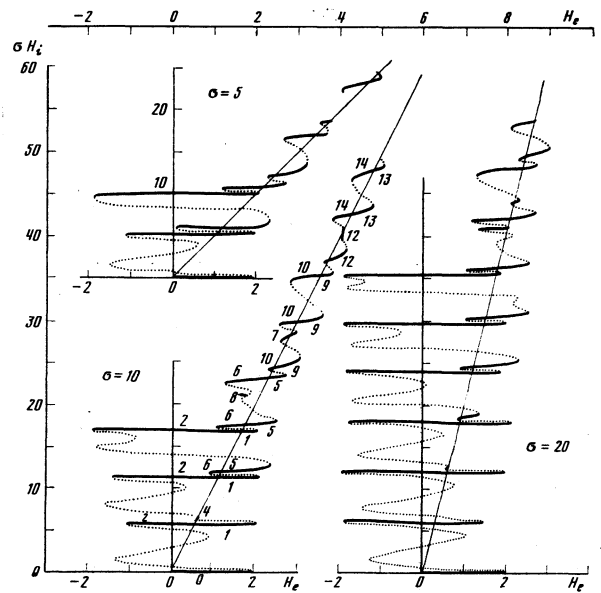


FIG. 4. The same as in Fig. 2, but at  $L=5$ .

numbers on the curves in Fig. 6 represent different solutions, the number  $N$  of the solution being connected with the number  $n$  in one of the following manners:  $N = 4n, N = 4n + 1, N = 4n + 2, N = 4n + 3$ , and an increase of  $n$  by unity corresponds to entry of an additional vortex into the junction (see Ref. 16 for details of the assumed classification of the solutions). The primes in Fig. 6 mark the numbers corresponding to bounded solutions [for which the constant  $C$  in (5) and (6) is negative and the field  $H(x)$  is of alternating sign]. In Figs. 2–4 are also indicated the numbers of the solutions that are realized at various positions of the representative point on the curves. A comparison of Figs. 2–4 with Fig. 6 makes it easy to trace the character of variation of the field  $H(x)$  in the junction when the external field  $H_e$  changes.

### 3. INVESTIGATION OF THE STABILITY OF THE SOLUTIONS

We check on the stability of the solutions corresponding to different positions of the representative point on the curves of Figs. 2–4 by the method used by us previously for other problems.<sup>11–18</sup> We choose as the

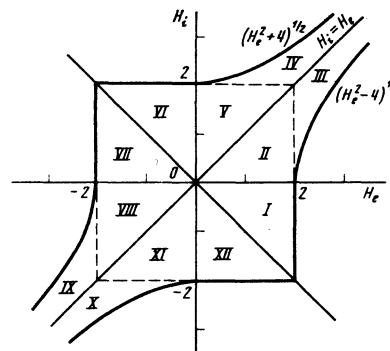


FIG. 5. Regions of existence of static solutions.

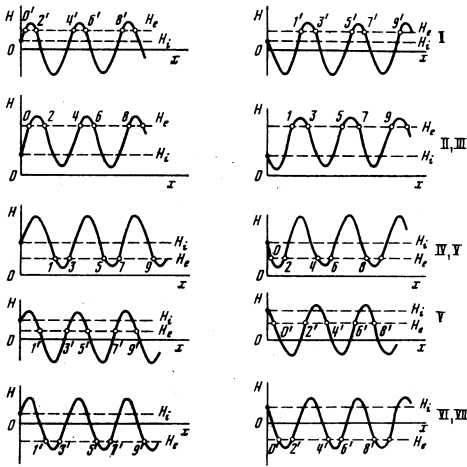


FIG. 6. Schematic form of the configurations of the field  $H(x)$  realized in a junction of finite width in different regions of variation of the parameters  $H_i$  and  $H_e$  (see Fig. 5). The numbers on the curves correspond to different solutions. The primed numbers are those of the bounded solutions (for which the field  $H(x)$  belongs to an alternating-sign branch).

basis the nonstationary equation

$$\frac{d^2\varphi}{dt^2} + \beta \frac{d\varphi}{dt} - \frac{d^2\varphi}{dx^2} + \sin\varphi = 0, \quad (11)$$

which describes the evolution of the solution with time (here is  $\beta$  is a phenomenological parameter that takes the damping into account and ensures a static solution as  $t \rightarrow \infty$ ). Putting  $\varphi(x, t) = \varphi(x) + \psi(x)e^{\omega t}$ , we obtain a linearized equation for the Fourier component of the small deviation ( $\psi \ll 1$ ) from the investigated static solution  $\varphi(x)$ :

$$d^2\psi/dx^2 - \cos\varphi(x)\psi = E\psi, \quad E = \omega^2 + \beta\omega. \quad (12)$$

Equation (12), together with the boundary conditions that follow (2) and (4)

$$d\psi/dx|_{x=0} = \varphi(0)/\sigma, \quad d\psi/dx|_{x=L} = 0, \quad (13)$$

determines the spectrum of the eigenvalues  $E$ . If at least one of the eigenvalues  $E$  is positive, then the growth rate of the solution  $\omega_+ = -\frac{1}{2}\beta + (\frac{1}{4}\beta^2 + E)^{1/2} > 0$  is positive and the deviation  $\psi e^{\omega_+ t}$  increases with time, thus indicating that the solution  $\varphi(x)$  is unstable. On the other hand, if all the eigenvalues  $E < 0$ , then the deviation  $\psi e^{\omega t}$  decreases with time and the solution is stable.

The system (12), (13) was investigated by us numerically with a computer. By specifying the values  $\varphi(0)$  and  $H_i = \varphi(0)/\sigma$ , we found the static solution  $\varphi(x)$  of Eq. (1), and then solved the problem (12), (13) for the minimal positive eigenvalue. The results of this investigation can be formulated in the following manner.

In Figs. 2-4, all the descending branches of the curves (for which the values of  $H_i$  decrease with increasing  $H_e$ ) are unstable. Among the ascending (with increasing  $H_e$ ) branches, the unstable ones are almost all the branches corresponding to bounded ( $C < 0$ ) solutions (for example, the ascending branches 1', 2', 3' in Figs. 2-4 are unstable).<sup>4</sup> In addition, there are unstable branches also among the growing solutions

( $C < 0$ ) (for example, branch 8 in Fig. 4, marked by an arrow, is also unstable). The remaining points of the  $H_i(H_e)$  curves correspond to stable solutions. Thus, the sequence of the appearance of the stable and unstable regions at  $L > 3$  is quite complicated.

#### 4. FREE ENERGY OF STATES. HYSTERESIS

A useful characteristic of the state of a system is its free energy  $G$ . There is a well known expression for the functional of the free energy of a weak superconductor in an external magnetic field in the absence of current.<sup>1</sup> This expression was generalized in Ref. 17 to include the case when transport current flows in the system. In our case, to find the functional  $G$  it is necessary to take into account also the presence in the system of a cavity with a magnetic field. This can be quite simply done. It has already been noted that Eq. (1) for the phase  $\varphi$  coincides in this case with the equation for the flux in the system [relation (3)]. It is clear that from the mathematical point of view the solution of the boundary value problem (1), (2), and (4) should be an extremal of the functional of the free energy, i.e., the condition  $\delta G = 0$  should be satisfied on the solution  $\varphi(x)$ . Taking this into account, we easily obtain<sup>5</sup>

$$G[\varphi] = \mathcal{E}[\varphi] + \frac{1}{2}\varphi_0 H_i - \varphi_L H_e, \\ \mathcal{E}[\varphi] = \int_0^L \left[ \frac{1}{2} \left( \frac{d\varphi}{dx} \right)^2 + 1 - \cos\varphi \right] dx, \quad (14) \\ \varphi_0 = \varphi(0), \quad \varphi_L = \varphi(L).$$

This expression can also be obtained from (11). In addition, from (11) we can find, with the aid of simple transformations (see Ref. 17 for details), for example, the law governing the change of the energy of a weak superconductor in our system:

$$\frac{d\mathcal{E}[\varphi(t)]}{dt} = H_e(t)E_e(t) - \frac{d}{dt} \left( \frac{\sigma H_i^2(t)}{2} \right) - \beta \int_0^L \left( \frac{d\varphi}{dt} \right)^2 dx, \quad (14a) \\ \mathcal{E}[\varphi(t)] = \int_0^L \left[ \frac{1}{2} \left( \frac{d\varphi}{dt} \right)^2 + \frac{1}{2} \left( \frac{d\varphi}{dx} \right)^2 + 1 - \cos\varphi \right] dx.$$

The first term in the right-hand side of (14a) can be naturally interpreted as the Poynting vector at the point  $x = L$ , while the second term is simply the change of the energy of the magnetic field in the cavity, and the third describes the energy dissipation in the junction.

With the aid of (14) we can compare the free energies of the different states and determine the points of the equilibrium transition from one stable state to another (assuming that the system follows all the time the states with the minimal free energy). An example of the function  $G[\varphi]$  for several states is shown in Fig. 7. The arrows in Figs. 2-4 indicate the points  $H_{eq}$  of the equilibrium transition from one stable state to another. The fact that at a given external field  $H_e$  there can exist in a system several stable states make hysteresis phenomena possible. The system can then be in a state with free energy exceeding the minimum possible (for example, the stable states 0' on Figs. 2 and 7 have at  $H_e > H_{eq}$  are larger free energy than the states 1 and 2). The boundaries of the hysteresis, obviously, coincides with the boundaries of the existence of the corresponding stable state and lie inside the hyperbolas  $H_i = (H_e^2$

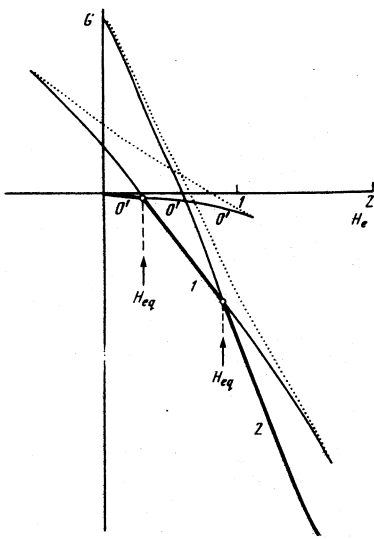


FIG. 7. Dependence of the free energy  $G$  on  $H_e$  for a SQUID with  $L=1$  and  $\sigma=10$ . The arrows indicate the points  $H_{eq}$  of the equilibrium transition from one solution to another. The numbers on the curves correspond to the numbering system used for the solutions in (6) (not all the solutions are marked).

$\pm 4)^{1/2}$  that bound in Fig. 5 the regions of existence of the static solutions.

We call attention to two types of hysteresis states. The first is connected with the penetration of the field inside the ring in quantized batches, whereby no qualitative change takes place in the field configuration in the junction itself (the transitions  $0'$  (region II)  $\rightarrow 0$  (region V) and  $1$  (region II)  $\rightarrow 2$  (region V) in Fig. 2 correspond to penetration of individual flux quanta inside the ring opening).

Another type of state is connected with the penetration of the flux quantum with the formation of a vortex inside the junction itself (transitions  $1$  (region II)  $\rightarrow 6$  (region V) in Fig. 3). With increasing  $L$ , such states appear more frequently (Fig. 4). At sufficiently small  $L$  there is no hysteresis at all<sup>1-3</sup> and states with vortices in the junction itself are also impossible (the vortex does not fit in the junction if the field is not very strong).

We note that in the absence of an external field ( $H_e = 0$ ) states with a flux "frozen-in" inside the ring are possible in our system (see Figs. 2-4). In a singly connected system (wide junction in an external field<sup>12</sup>) at  $H_e = 0$  there were no hysteresis states and the only solution corresponded to the case  $H(x) = 0$ . Thus, allowance for the inhomogeneity in the system [the presence of an opening jointly with the condition of flux quantization (3)] leads to the appearance of the pinning effect and to the possibility of hysteresis states in a zero field (see also Ref. 9).

## 5. ASYMPTOTIC EXPRESSIONS AND DISCUSSION OF RESULTS

In a number of limiting cases it is possible to obtain analytic expressions that yield the solution of the problem. Thus, in the case of a narrow junction ( $L \ll 1$ ) the fields inside and outside the ring are almost equal,  $|H_e$

$-H_i| \ll 1$ . Expanding the integral in (10) in powers of the small parameter  $H_e - H_i$ , we get  $L \approx (H_e - H_i)/\sin \sigma H_i$ , whence

$$H_e = H_i + L \sin \sigma H_i. \quad (15)$$

This formula is suitable in a large range of fields  $H_e$ , but such that do not violate the condition  $LH_e \ll 1$ . Calculating the derivative of (15) we get

$$dH_e/dH_i = 1 + L\sigma \cos \sigma H_i, \quad (16)$$

i.e., at  $L\sigma < 1$  we have  $dH_e/dH_i > 0$  and there is no hysteresis on the  $H_i(H_e)$  curves. On the other hand, if  $L\sigma > 1$ , then the derivative  $dH_e/dH_i$  can be either positive or negative, and the  $H_i(H_e)$  curves should have sections with hysteresis. It is easy to show that the stability limit of the solutions (i.e., the point  $E = 0$ , see Sec. 3) is determined at  $L \ll 1$  by the condition  $dH_e/dH_i = 0$ , i.e.,  $\cos \sigma H_i = -1/\sigma L$ . At  $\sigma L < 1$  all the states are stable.

In the case of arbitrary  $L$  but strong fields ( $H_e \gg 1$ ), we have  $\varphi_L - \varphi_0 \approx H_i L$  and, in addition,  $H_e \approx H_i$ . After elementary trigonometric transformations we obtain from (8), taking (4) into account,

$$H_e = H_i + \frac{2}{H_i} \sin \left[ H_i \left( \frac{L}{2} + \sigma \right) \right] \sin \left( \frac{H_i L}{2} \right). \quad (17)$$

It is easy to verify that in fields  $H_i > L + \sigma \gg 1$  there is no hysteresis on the  $H_i(H_e)$  plot. In weaker fields (but, as before,  $H_e \gg 1$ ), hysteresis is possible. The function  $H_i(H_e)$  can be easily constructed graphically from the asymptotic formulas (15) and (17) (see Fig. 8). The product of the sine functions in (17) is typical of the beats produced when oscillations are superimposed (the analogy with an oscillating system explains the use of the term "quantum interference"). If the quantities  $L$  and  $\sigma$  are commensurate (their ratio is rational), then the product of the sine functions is a periodic function. For noncommensurate values of  $L$  and  $\sigma$  there is no periodic dependence in formula (17).

We call attention to the fact that formula (15) yields an oscillatory function  $H_i(H_e)$  with a constant oscillation amplitude. According to (17), in strong fields the amplitude of the oscillations decreases in inverse proportion to  $H_e$  and the best picture connected with formation of vortices inside the transition sets in.

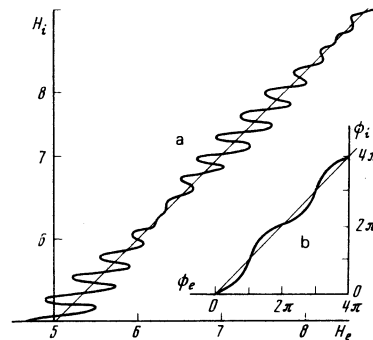


FIG. 8. a) Asymptotic plot of formula (17) for  $L=3$ ,  $\sigma=100$ , and  $H_e \gg 1$ . The curve has sections both with and without hysteresis (i.e., sections with single-valued  $H_i(H_e)$  dependence). The inset b shows a plot of (15) [or (20)] in the case  $l = \sigma L = 0.2$ . There is no hysteresis on this curve.

When the results obtained above are compared with the results of earlier work on the same subject,<sup>4-8</sup> it must be borne in mind that Refs. 4-8 dealt with a ring interferometer with a point contact ( $L \ll 1$ ). The analysis there was based on the phenomenological formula (in dimensionless units)

$$\phi_i = \phi_e - l j_{scr}, \quad (18)$$

which states that the magnetic flux  $\phi_i$  inside the ring is equal to the external flux through the ring ( $\phi_e = H_e \sigma$ ) from which we subtract the flux connected with the screening current  $j_{scr}$  that flows around the ring (the Meissner effect). In formula (18) we have introduced a phenomenological parameter  $l$  (the coefficient of self induction of the ring), which remains undetermined. The quantity  $j_{scr} = I_{scr}/I_c$ , using the relations

$$I_{scr} = j_c \int_0^L \sin \varphi dx, \quad I_c = j_c L,$$

can be represented in the form

$$j_{scr} = \frac{1}{L} \int_0^L \sin \varphi dx = \overline{\sin \varphi} \quad (19)$$

and at small  $L$  we have  $j_{scr} = \sin \varphi(x) = \sin \varphi(0) \equiv \sin \phi_i$  {we make allowance here for the fact that the phase  $\varphi(0)$  is the dimensionless flux  $\phi_i$  inside the ring, [see (3)]}. As a result, Eq. (18) takes the form

$$\phi_i = \phi_e - l \sin \phi_i, \quad (20)$$

which coincides with Eq. (15) if the latter is multiplied by  $\sigma$  and we put  $l = \sigma L$ . We shall show that the last identity holds true in the general case for a barrier of arbitrary width  $L$ . In fact, from (18) and (19) we have

$$l = \frac{\phi_e - \phi_i}{j_{scr}} = \sigma (H_e - H_i) / \frac{1}{L} \left( \left. \frac{d\varphi}{dx} \right|_L - \left. \frac{d\varphi}{dx} \right|_0 \right) = \sigma L,$$

where we have used Eq. (1) and took into account the boundary conditions (2) and (4) for the field  $H$ .

Thus, the self-induction coefficient of a single ring interferometer is in the general case (in dimensionless units) equal to the product of the area of the opening by the width of the contact:

$$l = \sigma L. \quad (21)$$

Proceeding to dimensional units (see footnote 2), we obtain an expression for the dimensional self-induction coefficient  $\mathcal{L}$ :

$$\mathcal{L} = \frac{\Phi_0}{2\pi} \frac{\pi r^2}{\lambda_c^2 \Lambda_j}, \quad (22)$$

in which we express (18) in the form  $\Phi_i = \Phi_e - \mathcal{L} I_{scr}$ , where  $\Phi_{e,i}$  are dimensional fluxes and  $I_{scr}$  is the total current flowing around the ring.

Let us explain why the approach developed by us makes it possible to determine completely the parameter  $l$  (or  $\mathcal{L}$ ). The point is that we base ourselves essentially on Eq. (1), which connects the values of the field inside and outside the ring. The screening properties of the system are then automatically taken into account by the form of Eq. (1), and the weakening of the internal field (the Meissner effect) is determined in our case completely by the geometric factors  $L$  and

$\sigma$ . In the earlier papers<sup>4-8</sup> and in Eq. (18), there was actually no use made of Eq. (1), and the Meissner effect was taken into account phenomenologically by introducing a certain (indeterminate coefficient  $l$ ).

Thus, our formula (15), when (21) is taken into account, coincides with formula (20) previously obtained for point contacts.<sup>4-8</sup> The condition for the applicability of this formula was indicated above, namely  $LH_e \ll 1$ . In sufficiently strong fields ( $H_e > 1/L$ ), even in the case of a point contact, a deviation from relation (20) takes place and it is necessary to use in its place Eq. (17). The latter is valid (at  $H_i \approx H_e \gg 1$ ) also for broad contacts and takes into account the effect of vortex formation inside the junction itself.

We note that the present paper did not deal with the nonstationary processes in the system. These can be analyzed in principle with the aid of the general equation (11), which in this case holds for the magnetic flux inside the system. The final state of the system, of course, depends here on the initial conditions. The establishment of the stationary state in a system with a point contact ( $L \ll 1$ ) was considered previously in a number of papers (see, e.g., Refs. 6-8). We note also that the nonstationary equation used in the cited papers for the magnetic-field flux in the system can be either obtained from (11) by averaging the last equation over the interval  $0 \leq x \leq L$  and then putting  $L \ll 1$ .

We note in conclusion the following circumstance. A ring SQUID in an external static field is always in one of the possible stable states and cannot be transformed by simply increasing the field into a nonstationary regime similar to that which arises in a Josephson contact when a current exceeding the critical value is made to flow through it. It is possible, however, to point out a situation wherein a nonstationary regime of this kind can be realized under static conditions. In fact, if the ring SQUID is made of two different superconductors and the points of their junctions are at different temperatures  $T_1$  and  $T_2$ , then an additional thermoelectric current is produced in such a ring, and with it is associated a magnetic flux  $\Phi_T$  (for more details see the review<sup>19</sup>). This magnetic flux is due to the disequilibrium (temperature gradient) and therefore is not subject to the quantization condition (i.e., it can assume arbitrary values). Therefore when a bimetallic SQUID is heated the field  $H_i$  in its internal cavity increases and can in principle go outside the limits of the hyperbolas  $H_i = (H_e^2 \pm 4)^{1/2}$  (see Fig. 5) that bound the limit of the existence of the static solutions. The SQUID then goes over into a nonstationary regime, a traveling vortex structure is produced in the junction, and the SQUID itself serves as a source of electromagnetic radiation (for details see Ref. 14, where a nonstationary picture of this type is considered). We note that in a sufficiently strong external field the hyperbolas  $(H_e \pm 4)^{1/2}$  are close to one another and therefore the appearance of a weak thermoelectric flux may be sufficient to transfer the SQUID into a nonstationary regime.

In conclusion we thank V.V. Shmidt for a discussion of the results.

- <sup>1</sup>The term SQUID stands for "superconducting quantum interference device."
- <sup>2</sup>In dimensional variables, these inequalities take the form  $L \ll \lambda_J$  and  $L \gg \lambda_J$ , where  $\lambda_J \sim 0.1$  mm is the Josephson depth of penetration. In the text we use dimensionless quantities, with the lengths measured in units of  $\lambda_J$ , the current in units of  $j_c$  ( $j_c$  is the maximum value of the stationary current through the barrier), the field in units of  $H_J = \Phi_0/2\pi\lambda_J\Lambda \sim 1$  ( $\Phi_0$  is the flux quantum,  $\Lambda = 2\lambda_L + l$ ,  $\lambda_L$  is the London penetration depth,  $l \sim 10^{-7}$  cm is the thickness of the dielectric layer, and the flux in units of  $\Phi_0/2\pi$ ).
- <sup>3</sup>The numbering of the regions I–XII in Fig. 5 was chosen to preserve the correspondence with the numbering assumed previously<sup>16</sup> in the investigation of the behavior of a Josephson barrier with current in an external field.
- <sup>4</sup>This agrees with the fact that the solutions with alternating-sign sections of the field  $H(x)$  turned out to be unstable also in the previously considered problems.<sup>12–14</sup> The ascending branches of the solutions  $0'$ , however, are stable.
- <sup>5</sup>The term  $\frac{1}{2}\varphi_0 H_i$  in (14) (equal to  $\sigma H_i^2/8\pi$  in dimensional units) is the energy of the magnetic field inside the cavity. The expression for the free energy of a singly connected weak superconductor in an external field<sup>14,17</sup> contains a term  $H_c^2/4\pi$ , therefore the coefficient  $\frac{1}{2}$  is missing from the corresponding term.
- <sup>1</sup>I. O. Kulik and I. K. Yanosn, *Éffekt Dzhosefsona v sverkhprovodyashchikh tunnel'nykh strukturakh* (Josephson Effect in Superconducting Tunnel Structures), Nauka, 1970.
- <sup>2</sup>L. Solymar, *Superconductive Tunneling and Applications*, Wiley, 1972.
- <sup>3</sup>K. K. Likharev and B. T. Ul'rikh, *Sistemy s dzhosefsonovskimi kontaktami* (Systems with Josephson Junctions), Moscow Univ. Press, 1978.
- <sup>4</sup>A. H. Silver and J. E. Zimmerman, *Phys. Rev.* **157**, 317 (1967).
- <sup>5</sup>A. M. Goldman, *J. Low Temp. Phys.* **3**, 55 (1970).
- <sup>6</sup>H. J. T. Smith and J. A. Blackburn, *Phys. Rev.* **B12**, 940 (1975).
- <sup>7</sup>T. C. Wang and R. I. Gayley, *Phys. Rev.* **B15**, 3401 (1977).
- <sup>8</sup>J. A. Blackburn, H. J. T. Smith, and V. Klein, *Phys. Rev.* **B15**, 4211 (1977).
- <sup>9</sup>V. V. Schmidt, *Solid State Comm.* **20**, 295 (1976).
- <sup>10</sup>V. V. Schmidt and V. G. Stel'makh, *Fiz. Nizk. Temp.* **3**, 1508 (1977) [*Sov. J. Low Temp. Phys.* **3**, 722 (1977)].
- <sup>11</sup>G. F. Zharkov, *Zh. Eksp. Teor. Fiz.* **71**, 1951 (1976) [*Sov. Phys. JETP* **44**, 1023 (1976)].
- <sup>12</sup>G. F. Zharkov and S. A. Vasenko, *ibid.* **74**, 665 (1978) [**47**, 350 (1978)].
- <sup>13</sup>S. A. Vasenko and G. F. Zharkov, *ibid.* **75**, 180 (1978) [**48**, 89 (1978)].
- <sup>14</sup>G. F. Zharkov and A. D. Zaikin, *Fiz. Nizk. Temp.* **4**, 586 (1978) [*Sov. J. Low Temp. Phys.* **4**, 283 (1978)].
- <sup>15</sup>G. F. Zharkov, *Zh. Eksp. Teor. Fiz.* **75**, 2196 (1978) [*Sov. Phys. JETP* **48**, 1107 (1978)].
- <sup>16</sup>G. F. Zharkov, *Proc. 20th All-Union Conf. on Low Temp. Phys.*, Moscow, part III, 1979, p. 257.
- <sup>17</sup>G. F. Zharkov and A. D. Zaikin, *Kr. soobshch. po fizike FIAN*, No. 7, 21 (1978).
- <sup>18</sup>G. F. Zharkov and A. D. Zaikin, *Proc. 20th All-Union Conf. on Low Temp. Phys.*, Moscow, part III, 1979, p. 259.
- <sup>19</sup>V. L. Ginzburg and G. F. Zharkov, *Usp. Fiz. Nauk* **125**, 19 (1978) [*Sov. Phys. Usp.* **21**, 381 (1978)].

Translated by J. G. Adashko

## Critical phenomena in thin superconducting films

I. Ya. Fogel', A. S. Sidorenko, L. F. Rybalchenko, and I. M. Dmitrenko

*Physicotechnical Institute of Low Temperatures, Ukrainian Academy of Sciences*

(Submitted 22 January 1979)

*Zh. Eksp. Teor. Fiz.* **77**, 236–249 (July 1979)

Resistive transitions occurring in thin vanadium films with varying temperature, current, and magnetic field were investigated. It was observed that the excess conductivity  $\sigma'$  at  $T < T_c$  and  $H < H_c$  depends exponentially on the reduced parameters  $\epsilon = 1 - T/T_c$ ,  $h = 1 - H/H_c$ , and  $j = 1 - I/I_c$ . The resistive transitions satisfy the similarity law, i.e., they can be described by functions of  $\epsilon$ ,  $h$ , and  $j$  which are universal for all the curves. The obtained regularities are discussed within the framework of the fluctuation theory of second-order phase transitions. The temperature and magnetic-field widths of the transition agree numerically with the predictions of the theory.

PACS numbers: 73.60.Ka, 74.40.+k

Resistive transitions in the region of phase transformations into the superconducting state are measured quite frequently. These measurements determine the values of the critical parameters—the temperature of the superconducting transition  $T_c$  and the critical magnetic fields  $H_c$ . However, the nature of the resistive state in the region of the superconducting transition is as yet nowhere clear.

In the vicinity of the phase-transition point, a substantial role is played by fluctuations of the order parameter, which lead to noticeable deviations from the self-consistent field theory (SFT), which makes use of an

average value of the order parameter  $|\Delta|^2$ . In the critical region defined by the so-called Ginzburg number,<sup>1</sup> where the fluctuation corrections exceed the mean value of  $|\Delta|^2$ , the SFT cannot be used at all and an adequate description is obtained within the framework of similarity theory (see, e.g., the monograph of Patashinskii and Pokrovskii<sup>2</sup>).

The corrections that must be introduced in the SFT when the critical region is approached can be obtained from an analysis of the small fluctuations. In particular, the result of their contribution is an excess conductivity at  $T \gg T_c$ , first calculated by Aslamazov and